Proceedings of the Conference on Computational Engineering and Science JSCES
Vol. 29, Jun. 2024

On the formulation of topology optimization for finite strain elastoplastic materials

Jike Han [1)], Kozo Furuta [2)], Tsuguo Kondoh [3)], Shinji Nishiwaki [3)], Kenjiro Terada [1)]

[1)] International Research Institute of Disaster Science, Tohoku University (E-mail: jike.han.e1@tohoku.ac.jp)
[2)] Department of Micro Engineering, Kyoto University
[3)] Department of Mechanical Engineering and Science, Kyoto University

We present a unified formulation of topology optimization formulation for finite strain elastoplastic materials. As the primal problem to describe the elastoplastic behavior, we consider the standard J_2-plasticity model incorporated into Neo-Hookean elasticity. For the optimization problem, the objective function is set to accommodate multiple objectives, and the continuous adjoint method is employed to derive the sensitivity. In addition, the reaction-diffusion equation is used to update the design variable in an optimizing process. Several numerical examples are presented to demonstrate the ability of the proposed formulation.

Key Words : *Topology optimization, Finite strain, Plasticity, Adjoint method*

1. INTRODUCTION

Optimization problems that maximize objectives within finite resources and certain constraints have been studied in various research fields. Particularly in the structural engineering community, scholars have pursued finding a better structure with a reasonable amount of materials while maintaining the capability. To support this challenge, topology optimization [1] has received attention in these two or three decades.

In particular, topology optimization of elastoplastic materials has become popular in the last decade. As far as we know, while around twenty papers have been published, all of them were developed within the small strain framework. Considering that elastoplastic materials usually can withstand large deformation, a formulation based on the finite strain framework should be addressed. However, only a few studies [2,3,4,5] are available nowadays. Also, there is no formulation that allows for arbitrary objectives to be considered, and thus, this is an interesting topic to tackle.

Meanwhile, many studies use spatial and temporal discretization (discrete adjoint method) to derive the sensitivity of elastoplastic topology optimization problems. Probably, this is due to the difficulty of deriving sensitivities due to the complexity of the governing equations. However, from the overall insight of continuum mechanics, this discretization-dependent formulation is somewhat tricky. For that reason, we can pursue a formulation for elastoplastic topology optimization that does not rely on discretization.

In this context, this study presents a formulation of elastoplastic topology optimization within the framework of finite strain theory. As the primal problem to describe the elastoplastic behavior, we consider the standard J_2-plasticity model incorporated into Neo-Hookean elasticity. For the optimization problem, the objective function is set to accommodate multiple objectives, and the continuous adjoint method is employed to derive the sensitivity. In addition, the reaction-diffusion equation is used to update the design variable in an optimizing process. Several numerical examples are presented to demonstrate the ability of the proposed formulation.

2. FORMULATION

(1) Governing equations of primal problem

As the primal problem to describe elastoplastic responses of materials, we postulate the following governing equations:

$$\left.\begin{aligned} &\nabla \cdot \boldsymbol{P} + \boldsymbol{B} = \rho_0 \ddot{\boldsymbol{u}} \text{ in } \mathcal{B}_0, \\ &\boldsymbol{P} \cdot \boldsymbol{N} = \bar{\boldsymbol{T}} \text{ on } \partial\mathcal{B}_0^N,\ \boldsymbol{u} = \bar{\boldsymbol{u}} \text{ on } \partial\mathcal{B}_0^D \\ &\Phi^{\mathrm{p}} = \|\boldsymbol{\tau}_{\mathrm{dev}}\| - \sqrt{\frac{2}{3}}\,(y_0 + r^{\mathrm{p}}) \le 0, \\ &\quad \gamma^{\mathrm{p}} \ge 0,\ \Phi^{\mathrm{p}}\gamma^{\mathrm{p}} = 0 \text{ in } \mathcal{B}_0 \\ &\mathfrak{n} - \frac{\boldsymbol{\tau}_{\mathrm{dev}}}{\|\boldsymbol{\tau}_{\mathrm{dev}}\|} = \boldsymbol{0} \text{ in } \mathcal{B}_0 \end{aligned}\right\} \forall t, \qquad (1)$$

where $\boldsymbol{P}$, $\boldsymbol{B}$, ρ_0, $\boldsymbol{N}$, $\bar{\boldsymbol{T}}$, and $\bar{\boldsymbol{u}}$ denote the first Piola-Kirchhoff stress tensor, body force vector, mass density, outward unit normal vector, prescribed traction force vector, and prescribed displacement vector, respectively. Also, Φ^{p}, $\boldsymbol{\tau}$, y_0, r^{p}, and $\mathfrak{n}$ are the plastic yield function, Kirchhoff stress tensor, initial yield stress, plastic hardening force, and flow tensor, respectively. Note that the following three variables are unknowns in the primal problem:

$$\begin{aligned} &\text{Displacement vector: } \boldsymbol{u}, \\ &\text{Plastic multiplier: } \gamma^{\mathrm{p}}, \quad \text{Flow tensor: } \mathfrak{n}. \end{aligned} \qquad (2)$$

(2) Optimization problem

Subsequently, we introduce a scalar-valued function $\omega(\boldsymbol{X}) \in [0,1]$ at a certain position $\boldsymbol{X} \in \mathcal{D}_0$ as a design variable and define the objective function $\mathcal{F}$ as

$$\begin{aligned}\mathcal{F}(\omega) = \int_t \Bigg(& \int_{\mathcal{B}_0} f_{\mathcal{B}_0}(\boldsymbol{u}, \boldsymbol{F}, \gamma^{\mathrm{p}}, \mathbf{n}, \omega)\,\mathrm{dV} \\ & + \int_{\partial\mathcal{B}_0^N} f_{\partial\mathcal{B}_0^N}(\boldsymbol{u}, \omega)\,\mathrm{dA} \\ & + \int_{\partial\mathcal{B}_0^D} f_{\partial\mathcal{B}_0^D}(\boldsymbol{F}, \omega)\,\mathrm{dA} \Bigg)\,\mathrm{dt},\end{aligned} \tag{3}$$

where $f_{\mathcal{B}_0}$, $f_{\partial\mathcal{B}_0^N}$, and $f_{\partial\mathcal{B}_0^D}$ denote the objective density functions inside the body ($f_{\mathcal{B}_0}$) and on the boundary surfaces ($f_{\partial\mathcal{B}_0^N}$ and $f_{\partial\mathcal{B}_0^D}$), respectively. Here, $\boldsymbol{F}$ denotes the deformation gradient tensor. It is noted that each of the objective density functions can consist of multiple sub-functions such that

$$\begin{aligned} f_{\mathcal{B}_0}(\boldsymbol{u}, \boldsymbol{F}, \gamma^{\mathrm{p}}, \mathbf{n}, \omega) &= \sum_{i=1} \zeta_i \tilde{f}_{\mathcal{B}_0,i}(\boldsymbol{u}, \boldsymbol{F}, \gamma^{\mathrm{p}}, \mathbf{n}, \omega), \\ f_{\partial\mathcal{B}_0^N}(\boldsymbol{u}, \omega) &= \sum_{i=1} \zeta_i \tilde{f}_{\partial\mathcal{B}_0^N,i}(\boldsymbol{u}, \omega), \\ f_{\partial\mathcal{B}_0^D}(\boldsymbol{F}, \omega) &= \sum_{i=1} \zeta_i \tilde{f}_{\partial\mathcal{B}_0^D,i}(\boldsymbol{F}, \omega), \end{aligned} \tag{4}$$

where $\tilde{f}_{\mathcal{B}_0,i}$, $\tilde{f}_{\partial\mathcal{B}_0^N,i}$, and $\tilde{f}_{\partial\mathcal{B}_0^D,i}$ denote i-th sub-functions, and ζ_i is the weight of i-th sub-function, respectively.

Assuming the plastic loading state, we formulate the optimization problem subject to Eq. (1). Under the general setting above, the optimization problem can be defined as

$$\underset{\forall\omega\in\mathcal{D}_0}{\text{Maximize}}\ \mathcal{F}(\omega) \ \text{ subject to Eq. (1) and } \bar{V} \le 0, \tag{5}$$

where the last inequality represents the volume constraint. It is noted that the elastic parameters (E, ν, ρ_0), the plastic paramaters (y_0, h, y_∞, β_{y}), and the prescribed traction force $\bar{\boldsymbol{T}}$ are dependent on the design variable ω in our formulation. As a common practice to remove the constraint conditions, we define the following Lagrangian:

$$\tilde{\mathcal{F}} = \int_t \left(\dot{\mathcal{F}} + \boldsymbol{\lambda} \diamond \boldsymbol{R} \right) \mathrm{dt} - \theta \bar{V}, \tag{6}$$

where $\boldsymbol{\lambda}$ and θ denote the generic Lagrange multipliers, and $\boldsymbol{R}$ corresponds to the set of functions in the governing equations in Eq. (1) that are supposed to be zero. Here, $\diamond$ is the inner product operator in a general sense.

(3) Governing equations of adjoint problem

As a preliminary step to apply the adjoint method to obtain the design sensitivity, the generic Lagrange multiplier is identified with the collection of adjoint variables defined as $\boldsymbol{\lambda} = \{\boldsymbol{w},\ \eta^{\mathrm{p}},\ \boldsymbol{\pi}\}$, where the components are the following variables:

$$\begin{gathered}\text{Adj. displacement vector: } \boldsymbol{w}, \\ \text{Adj. plastic multiplier: } \eta^{\mathrm{p}}, \quad \text{Adj. flow tensor: } \boldsymbol{\pi}.\end{gathered} \tag{7}$$

Here, the first variation of the Lagrangian $\tilde{F}$ in Eq. (6) with respect to the design variable $\omega(\boldsymbol{X})$ yields

$$\begin{aligned}\frac{\delta\tilde{\mathcal{F}}}{\delta\omega} = \frac{\delta_\omega\tilde{\mathcal{F}}}{\delta\omega} &+ \left[\frac{\partial\tilde{\mathcal{F}}}{\partial\boldsymbol{u}} \cdot \frac{\delta\boldsymbol{u}}{\delta\omega} + \frac{\partial\tilde{\mathcal{F}}}{\partial\nabla\boldsymbol{u}} : \nabla\frac{\delta\boldsymbol{u}}{\delta\omega}\right] \\ &+ \left[\frac{\partial\tilde{\mathcal{F}}}{\partial\gamma^{\mathrm{p}}}\frac{\delta\gamma^{\mathrm{p}}}{\delta\omega}\right] + \left[\frac{\partial\tilde{\mathcal{F}}}{\partial\mathbf{n}} : \frac{\delta\mathbf{n}}{\delta\omega}\right].\end{aligned} \tag{8}$$

Note that the three bracketed terms vanish as long as the solutions to the following adjoint problem are found:

$$\left.\begin{aligned}
&-\frac{\partial f_{\mathcal{B}_0}}{\partial\boldsymbol{u}} + \nabla\cdot\frac{\partial f_{\mathcal{B}_0}}{\partial\boldsymbol{F}} = \rho_0\boldsymbol{w}\cdot\frac{\partial\ddot{\boldsymbol{u}}}{\partial\boldsymbol{u}} \\
&-\nabla\cdot\left\{\boldsymbol{H} : \frac{\partial\boldsymbol{P}}{\partial\boldsymbol{F}} - \eta^{\mathrm{p}}\left(\frac{\partial\|\boldsymbol{\tau}_{\mathrm{dev}}\|}{\partial\boldsymbol{F}} - \sqrt{\frac{2}{3}}\frac{\partial r^{\mathrm{p}}}{\partial\boldsymbol{F}}\right)\right. \\
&\qquad \left. -\boldsymbol{\pi} : \left(\frac{\partial\mathbf{n}}{\partial\boldsymbol{F}} - \frac{\partial}{\partial\boldsymbol{F}}\frac{\boldsymbol{\tau}_{\mathrm{dev}}}{\|\boldsymbol{\tau}_{\mathrm{dev}}\|}\right)\right\} \ \text{in } \mathcal{B}_0 \\
&-\frac{\partial f_{\partial\mathcal{B}_0^N}}{\partial\boldsymbol{u}} - \frac{\partial f_{\mathcal{B}_0}}{\partial\boldsymbol{F}}\cdot\boldsymbol{N} \\
&= \left\{\boldsymbol{H} : \frac{\partial\boldsymbol{P}}{\partial\boldsymbol{F}} - \eta^{\mathrm{p}}\left(\frac{\partial\|\boldsymbol{\tau}_{\mathrm{dev}}\|}{\partial\boldsymbol{F}} - \sqrt{\frac{2}{3}}\frac{\partial r^{\mathrm{p}}}{\partial\boldsymbol{F}}\right)\right. \\
&\qquad \left. -\boldsymbol{\pi} : \left(\frac{\partial\mathbf{n}}{\partial\boldsymbol{F}} - \frac{\partial}{\partial\boldsymbol{F}}\frac{\boldsymbol{\tau}_{\mathrm{dev}}}{\|\boldsymbol{\tau}_{\mathrm{dev}}\|}\right)\right\}\cdot\boldsymbol{N} \ \text{ on } \partial\mathcal{B}_0^N \\
&\frac{\partial f_{\partial\mathcal{B}_0^D}}{\partial\boldsymbol{F}} = \boldsymbol{w}\cdot\frac{\partial\boldsymbol{T}}{\partial\boldsymbol{F}} \ \text{ on } \partial\mathcal{B}_0^D \\
&\frac{\partial f_{\mathcal{B}_0}}{\partial\gamma^{\mathrm{p}}} + \boldsymbol{H} : \frac{\partial\boldsymbol{P}}{\partial\gamma^{\mathrm{p}}} - \eta^{\mathrm{p}}\left(\frac{\partial\|\boldsymbol{\tau}_{\mathrm{dev}}\|}{\partial\gamma^{\mathrm{p}}} - \sqrt{\frac{2}{3}}\frac{\partial r^{\mathrm{p}}}{\partial\gamma^{\mathrm{p}}}\right) \\
&-\boldsymbol{\pi} : \left(-\frac{\partial}{\partial\gamma^{\mathrm{p}}}\frac{\boldsymbol{\tau}_{\mathrm{dev}}}{\|\boldsymbol{\tau}_{\mathrm{dev}}\|}\right) = 0 \ \text{ in } \mathcal{B}_0 \\
&\frac{\partial f_{\mathcal{B}_0}}{\partial\mathbf{n}} + \boldsymbol{H} : \frac{\partial\boldsymbol{P}}{\partial\mathbf{n}} - \eta^{\mathrm{p}}\frac{\partial\|\boldsymbol{\tau}_{\mathrm{dev}}\|}{\partial\mathbf{n}} \\
&-\boldsymbol{\pi} : \left(\mathbf{1}\overline{\otimes}\mathbf{1} - \frac{\partial}{\partial\mathbf{n}}\frac{\boldsymbol{\tau}_{\mathrm{dev}}}{\|\boldsymbol{\tau}_{\mathrm{dev}}\|}\right) = \mathbf{0} \ \text{ in } \mathcal{B}_0
\end{aligned}\right\} \ \forall t. \tag{9}$$

Here, we refer to $\boldsymbol{H}$ as the adjoint deformation gradient tensor.

(4) Sensitivity

As long as the adjoint variables in Eq. (7) are obtained as the solutions of Eq. (9), the first variation of the Lagrangian $\tilde{\mathcal{F}}$ in Eq. (8) is simplified as follows:

$$\frac{\delta\tilde{\mathcal{F}}}{\delta\omega} = \frac{\delta_\omega\tilde{\mathcal{F}}}{\delta\omega} = \frac{\partial\left\{\int_t\left(\dot{\mathcal{F}} + \tilde{\boldsymbol{\lambda}}\diamond\boldsymbol{R}\right)\mathrm{dt} - \theta\bar{V}\right\}}{\partial\omega}. \tag{10}$$

Then, the substitution of Eq. (1) and Eq. (3) into Eq. (10) leads to the sensitivities inside the body and on the Neu-

mann and Dirichlet boundaries as follows:

$$
\begin{aligned}
s_{\mathcal{D}_0} = \int_t \Bigg\{ & \frac{\partial f_{\mathcal{B}_0}}{\partial \omega} + \boldsymbol{H} : \frac{\partial \boldsymbol{P}}{\partial \omega} + \frac{\partial \rho_0}{\partial \omega} \boldsymbol{w} \cdot (\ddot{\boldsymbol{u}} - \boldsymbol{g}) \\
& - \eta^{\mathrm{p}} \left(\frac{\partial \| \boldsymbol{\tau}_{\mathrm{dev}} \|}{\partial \omega} \right. \\
& \left. - \sqrt{\frac{2}{3}} \left(\frac{\partial y_0}{\partial \omega} + \frac{\partial r^{\mathrm{p}}}{\partial \omega} \right) \right) \Bigg\} \mathrm{dt} - \theta \text{ in } \mathcal{D}_0, \qquad (11) \\
s_{\partial \mathcal{D}_0^N} = & \int_t \left(\frac{\partial f_{\partial \mathcal{B}_0^N}}{\partial \omega} - \boldsymbol{w} \cdot \frac{\partial \bar{\boldsymbol{T}}}{\partial \omega} \right) \mathrm{dt} \text{ on } \partial \mathcal{D}_0^N, \\
s_{\partial \mathcal{D}_0^D} = & \int_t \left(\frac{\partial f_{\partial \mathcal{B}_0^D}}{\partial \omega} - \boldsymbol{w} \cdot \frac{\partial \boldsymbol{T}}{\partial \omega} \right) \mathrm{dt} \text{ on } \partial \mathcal{D}_0^D.
\end{aligned}
$$

Here, the body force is replaced as $\boldsymbol{B} = \rho_0 \boldsymbol{g}$ with $\boldsymbol{g}$ being the gravitational acceleration vector. Note that the SIMP method is usd to interpolate material properties, and the reaction-diffusion equation are employed to update design variables.

3. NUMERICAL EXAMPLE

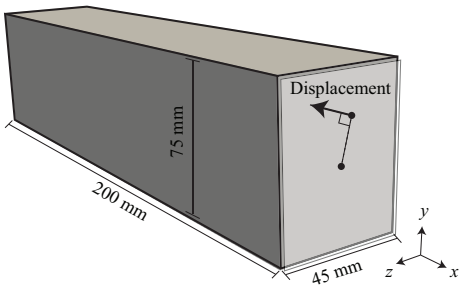

Fig. 1: Geometry and boundary conditions.

The plastic hardening maximization problem under the quasi-static condition is demonstrated here, for which the following objective function is considered:

$$
\begin{aligned}
\mathcal{F} = \zeta_1 \int_t \Bigg\{ & - \int_{\mathcal{B}_0} \boldsymbol{B} \cdot \boldsymbol{u} \mathrm{dV} - \int_{\partial \mathcal{B}_0^N} \bar{\boldsymbol{T}} \cdot \boldsymbol{u} \mathrm{dA} \\
& + \int_{\partial \mathcal{B}_0^D} \boldsymbol{T} \cdot \bar{\boldsymbol{u}} \mathrm{dA} \Bigg\} \mathrm{dt} \qquad (12) \\
+ \zeta_2 \int_t \int_{\mathcal{B}_0} & \left(y_0 \alpha + \int_0^{\alpha} r^{\mathrm{p}} \mathrm{d}\tilde{\alpha} \right) \mathrm{dV dt},
\end{aligned}
$$

Here, ζ_1 and ζ_2 are weights to control the contributions of two different objectives in the optimization problem.

The material distribution of a three-dimensional structure is optimized, whose geometries and boundary conditions are shown in Fig. 1. Here, forced displacements are applied to all nodes on the back and front surfaces so that torsion-bending coupled deformation occurs. In this example, dual phase 980 steel (DP980) and 5052 aluminum (Al5052) are chosen as the stronger and weaker materials, respectively. Except for the weights, all parameters needed to calculate this topology optimization are summarized in Table 1. While these parameters are kept fixed, three simulation cases (Case 1-3) are considered, i.e., $(\zeta_1, \zeta_2) = (1.00, 0.00),\ (0.17, 0.83),\ (0.00, 1.00)$. In addition, the initial value of the design variable is set to $\omega = 0.25$.

Fig. 2 shows the objective function-design iteration curves and error norm-design iteration curves, in which the gradual converging trends of the error norm and the improvements of the values of the objective functions are confirmed. Also, Fig. 3 shows the topologies obtained as the optimal solutions. From the top to bottom in each column of these figures, the distributions of the Al5052 (blue-colored region), Al5052 with plastic deformation (gray and blue-colored region), DP980 (red-colored region), DP980 with plastic deformation (gray and red-colored region), and both materials are shown. These figures show two distribution characteristics. For example, Case 1 confirms that the DP980 material is placed in the high stress region; see Fig. 3(a). Accordingly, as can be seen from the fourth row in each figure, the volume of the DP980 material with plastic deformation (gray and red-colored region) is the largest among the three cases. In addition, by increasing the value of ζ_2, the Al5052 material tends to be distributed in the region where plastic deformation occurs (gray and blue-colored region). Thus, the volume of the DP980 material with plastic deformation (gray and red-colored region) is decreased with the increase of ζ_2.

4. CONCLUSION

We have presented a topology optimization formulation for finite strain elastoplastic materials using the continuous adjoint method. Unlike previous studies on elastoplastic topology optimization problems, the proposed formulation does not require temporal and spatial discretizations and derives the governing equations and sensitivity of the adjoint problem based on the variational principle. Also, the form of the objective function allows multiple objectives to be considered in a single optimization process, which implies the generality of the proposed formulation. As the demonstration of the proposed formualtion, the plastic hardening maximization problem was identified as specific cases of the proposed formulation. Numerical examples show that the two-material optimization problems can be adequately solved under certain constraint conditions.

ACKNOWLEDGMENT This work was supported by JSPS KAKENHI Grant Number JP22K18755.

REFERENCES

[1] M. P. Bendsøe, N. Kikuchi, Generating optimal topologies in structural design using a homogenization method, *Comput. Methods Appl. Mech. Eng.* **71 (2)** (1988) 197–224. doi:10.1016/0045-7825(88)90086-2

[2] M. Wallin, V. Jönsson, E. Wingren, Topology optimization based on finite strain plasticity, *Struct. Multidiscip. Optim.* **54 (4)** (2016) 783–793. doi:10.1007/s00158-016-1435-0

[3] N. Ivarsson, M. Wallin, D. Tortorelli, Topology optimization of finite strain viscoplastic systems un-

Table 1: Simulation parameters.

Material parameter	DP980 / Al5052	Value	Unit
Young's modulus	E_{inc} / E_{mat}	225800 / 68900	[MPa]
Poisson's ratio	ν_{inc} / ν_{mat}	0.39 / 0.33	[-]
Initial yield stress	$y_{0,\mathrm{inc}}$ / $y_{0,\mathrm{mat}}$	609 / 210	[MPa]
Linear hardening parameter	h_{inc} / h_{mat}	0 / 0	[MPa]
Nonlinear hardening parameter	$y_{\infty,\mathrm{inc}}$ / $y_{\infty,\mathrm{mat}}$	1072 / 272	[MPa]
Saturation parameter	$\beta_{\mathrm{y,inc}}$ / $\beta_{\mathrm{y,mat}}$	76.4 / 38.8	[-]

Volume constraint parameter		Value	Unit
Allowance volume	$V_{\max}$	0.25	[-]
Initial saturation parameter	$\beta_{\mathrm{v},0}$	10	[-]
Maximum saturation parameter	$\beta_{\mathrm{v,max}}$	20	[-]
Increase ratio	m_{cof}	20	[-]

RDE parameter		Value	Unit
Length scale parameter	l_{d}	2.5	[mm]
Increment limit	$\bar{\omega}$	0.05	[-]
Alleviative coefficient	β_{s}	5	[-]
Convergence threshold	TOL.	20^{-4}	[-]

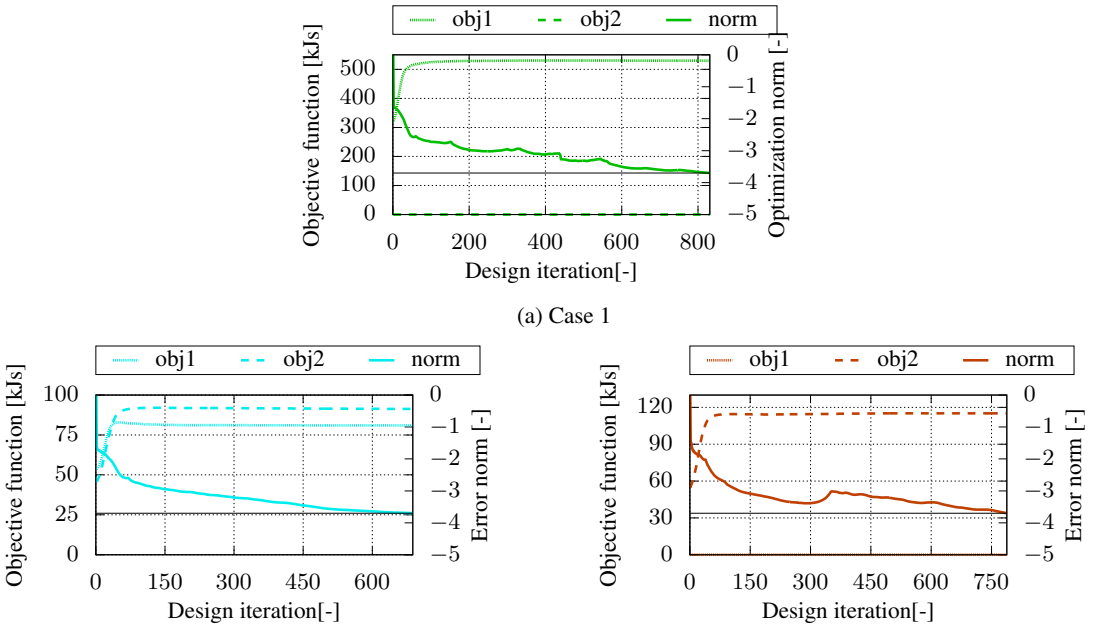

(a) Case 1

(b) Case 2

(c) Case 3

Fig. 2: Objective function-design iteration and error norm-design iteration curves. (Fine-dashed and coarse-dashed lines represent the histories of the first and second sub-objective functions whose weights are ζ_1 and ζ_2, respectively, and solid line represents the history of error norm. Black solid line is the convergence threshold.)

der transient loads, *Int. J. Numer. Methods Eng.* **114** (2018) 1351–1367. doi:10.1002/nme.5789

[4] N. Ivarsson, M. Wallin, O. Amir, D. A. Tortorelli, Plastic work constrained elastoplastic topology optimization, *Int. J. Numer. Methods Eng.* **122** (2021) 4354–4377. doi:10.1002/nme.6706

[5] G. Zhang, K. Khandelwal, Gurson-tvergaard-needleman model guided fracture-resistant structural designs under finite deformations, *Int. J. Numer. Methods Eng.* **123** (2022) 3344–3388. doi:10.1002/nme.6971

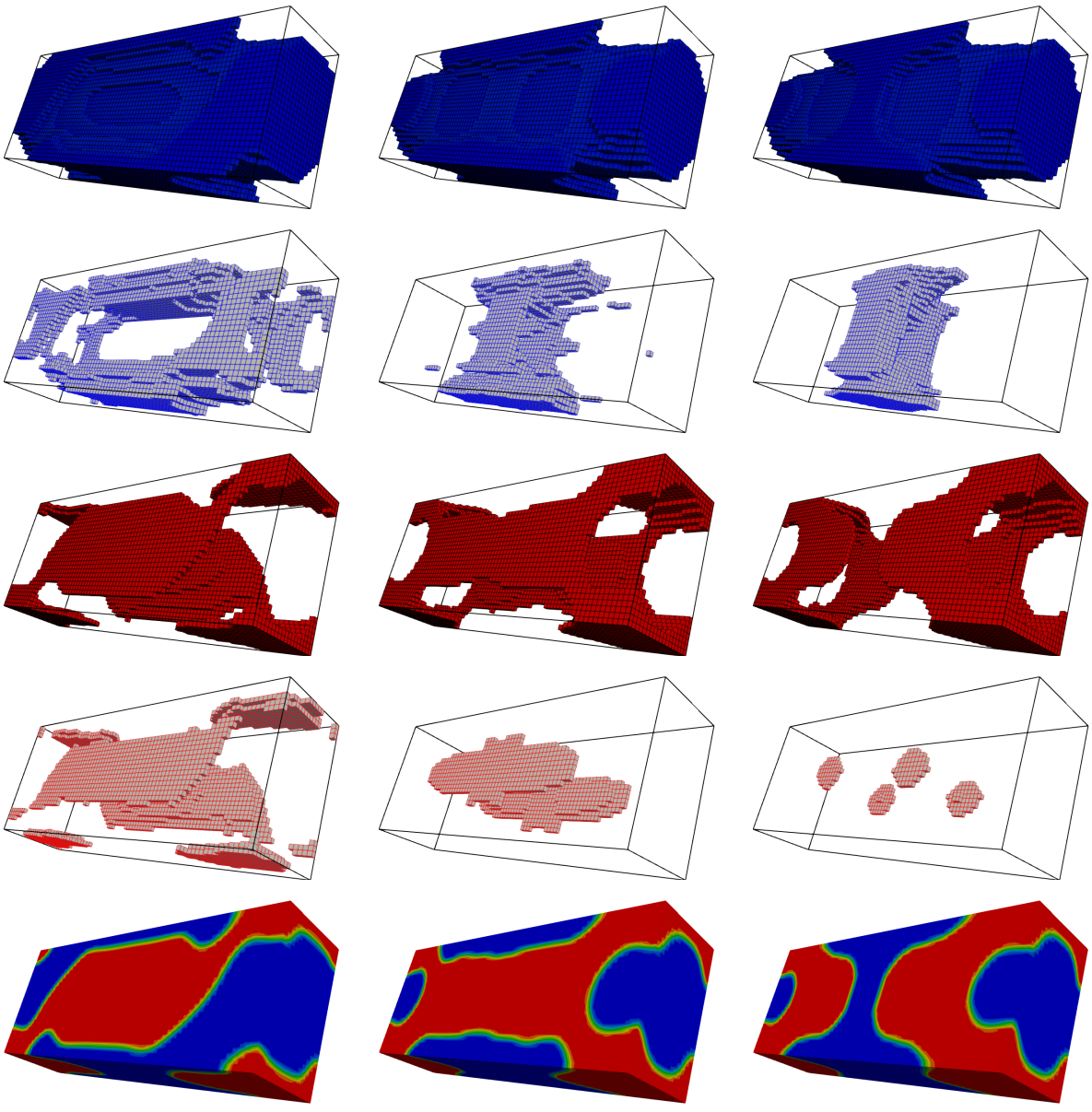

(a) Case 1 (b) Case 2 (c) Case 3

Fig. 3: Material distributions of Al5052 (blue-colored region) and DP980 (red-colored region), plastic deformation regions, and optimization results. (From the top to bottom in each column, the distributions of the Al5052, Al5052 with plastic deformation, DP980, DP980 with plastic deformation, and both materials are shown.)